Electrical nanogap devices for biosensing

For detecting substances that are invisible to the human eye or nose, and particularly those biomolecules, the devices must have very small feature sizes, be compact and provide a sufficient level of sensitivity, often to a small number of biomolecules that are just a few nanometres in size. Electrical nanogap devices for biosensing have emerged as a powerful technique for detecting very small quantities of biomolecules. The most charming feature of the devices is to directly transduce events of biomolecules specific binding into useful electrical signals such as resistance/impedance, capacitance/dielectric, or field-effect. Nanogap devices in electrical biosensing have become a busy area of research which is continually expanding. A wealth of research is available discussing planar and vertical nanogap devices for biosensing. Planar nanogap devices including label-free, gold nanoparticle-labeled, nanoparticles-enhanced, nanogapped gold particle film, and carbon nanotube nanogap devices as well as vertical nanogap devices with two and three terminals for biosensing are carefully reviewed. The aim of this paper is to provide an updated overview of the work in this field. In each part, we discuss the principles of operation of electrical biosensing and consider major strategies for enhancing their performance and/or key challenges and opportunities in current stages, and in their further development.

Xing Chen, Zheng Guo, Gui-Mei Yang, Jie Li, Min-Qiang Li, Jin-Huai Liu*, Xing-Jiu Huang*

The Key Laboratory of Biomimetic Sensing and Advanced Robot Technology, Anhui Province, Institute of Intelligent Machines, Chinese Academy of Sciences, Hefei 230031, PR China

*Correspondence should be addressed to X.-J. Huang and J.-H. Liu
 E-mail: xingjiuhuang@iim.ac.cn (X.J.H); jhliu@iim.ac.cn (J.H.L)

Electrical biosensors rely solely on the measurement of currents and/or voltages to detect binding[1,2]. Owing to its inherent superiorities of electrical transduction methods, such as excellent compatibility with advanced semiconductor technology, miniaturization, and low cost, biosensors based on electrical detection are capable of behaving at high performance with a simple miniaturized readout[3,4]. Nanogap electrodes are defined as a pair of electrodes with a nanometer gap[5]. Nano sized biomolecules can be trapped into a gap between two electrodes and connecting the electrodes; the biomolecules are therefore detected by observing their electrical behavior (resistance/impedance, capacitance/dielectric, or field-effect)[6].

By combining the unique electrical properties of nanoscale gaps, electrical detection systems supply excellent prospects for the design of biomolecular detection devices. Over the last 10 years, increased efforts have been made to establish nanogap biosensors which allow production of nanogap at reduced operation time and cost, as well as large-scale integrability, easy read-out and higher sensitivity.

It is important to point out that reviews dealing with nanogap issues mainly concentrate on the fabrication of nanogap electrodes[5], nanostructured-based electrical biosensors[7], and nanogap dielectric biosensor for label free DNA hybridization detection[6]. Very few papers have been written not only describing important contributions but also analysizing their possible properties. Here we review the progress so far in electrical nanogap biosensors, we survey available processing types suitable for the detection of different biomolecules, we discuss the principles of operation of electrical biosensing, and consider major strategies for enhancing their performance and/or key challenges and opportunities at their current stages and their further development.

Planar nanogap devices for biosensing
Label-free biosensing

Planar nanogap can be defined as both electrodes face each other horizontally in the device configuration (Fig. 1a). Some early reports were from UC Berkeley[8-11]. A nanogap was fabricated in which two polysilicon electrodes were separated from each other by a 50-100 nm
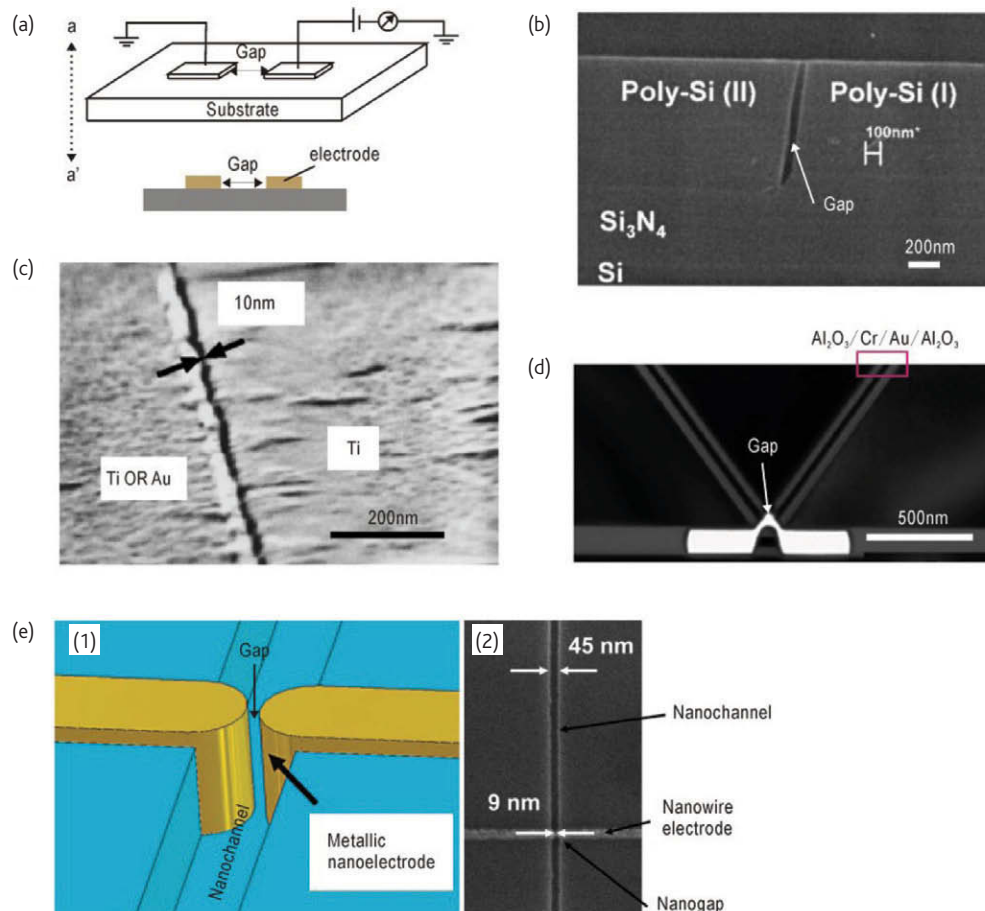

Fig. 1 Label-free planar nanogap devices for biosensing. a) Three-dimensional schematic and cross-section showing a planar nanogap structure. b) Nanogap using polysilicon as electrodes[11]. c) Nanaogap using two Ti electrodes or Ti/Au electrodes[15,16]. d) Trapezoid-shaped nanogap device fabricated using a silicon anisotropic wet etching technique on a silicon-on-insulator wafer[20]. e) A DNA detector with a nanogap inside a nanofluidic channel[21]. (1) A pair of metallic nanowires is formed across the nanochannel with a sub-10 nm breaking gap in the channel. (2) Top-view SEM image of a nanogap detector including a fluidic channel.

gap (Fig. 1b). Immobilized within each nanogap is a single strand of reference DNA. A voltage is then applied across the nanogap and a measurement is taken of the capacitance, and this is determined by the dielectric (insulating) property of the material in the nanogap, which changes as a result of hybridization.

However, as a result of the lack of rigidity, the immobilized oligonucleotides are randomly tangled, whereas a specific conformation is assumed when they hybridize with complementary DNA strands[12]. On the other hand, polysilicon electrodes suffer from a parasitic resistive layer caused by polycrystalline depletion effects, relatively low conductivity, and limitations in the types of self-assembled monolayers that are compatible with various biomolecules. Electrode materials with a good conductivity and biocompatibility should be studied[13].

One of the most important works on metal nanogap biosensors was by Dekker, et al.,[14] who studied the measurements of electrical transport through individual 10.4-nm-long, double-stranded poly(G)-poly(C) DNA molecules connected to two Pt nanoelectrodes (8 nm separation).

Hashioka, et al., fabricated flat metal nanogap DNA devices of sub-50 nm using conventional photolithograph (Fig. 1c). In earlier work[15], they detected DNA by using the metal nanogap devices (MNGDs) with two Ti electrodes, however, the electrical currents through the DNA in the MNGDs with two Ti electrodes are 1 nA or less, since DNA is not fixed on the surface of electrodes. In a more recent study[16], a nanogap between Au and Ti electrodes was used to detect DNA considering that DNA can be fixed on the Au electrodes by utilizing alkanethiol self-assembly monolayers[17]. Compared with the study using two Ti electrodes, the signal currents were increased more than ten fold.

Taking account of the biocompatible of gold materials, gold electrodes have been widely used in nanogap biodevices. Hwang and co-workers reported electrical transport through 60 base pairs of poly(dG)-poly(dC) (20.8-nm-long) DNA molecules[18]. The DNA solution is dropped and physically adsorbed in two gold electrodes with the gap of 20 nm (The size of the gap between two electrodes is comparable to the size of the length of the 60 base pairs). Iqbal, et al., reported dc measurements of covalently attached 18-mer thiolated ds-DNA in gold nanogaps to measure the electrical resistance of hybridized and denatured DNA molecules[19]. A dramatic decrease in conductance was observed, possibly suggesting complete or partial denaturing of the ds-DNA molecules bridging the nanogaps.

Although some bottom-up and top-down approaches have been used to produce some outstanding results, nanogap fabrication remains challenging because these methods still have disadvantages. For example, electron beam lithography, mechanical break junction, and electromigration methods are unsuitable for high-throughput fabrication. Electrochemical deposition methods have difficulty in providing well-defined patterns and thin film technology requires relatively complex fabrication processes. Furthermore, the widely used top-down approaches have to resolve issues such as high cost and low yield in order to be one step closer to routine fabrications.

Kim and co-workers used silicon anisotropic wet etching on a silicon-oninsulator (SOI) wafer to solve these problems[20]. Trapezoid-shaped nanogap (Fig. 1c) biosensors were fabricated for electrical and label-free detection of biomolecular interactions. The nanogap devices show a current increase when the proteins are bound to the surface. The current increases proportionally depending upon the concentrations of the molecules in the range of 100 fg/ml-100 ng/ml at 1 V bias.

An impressive research was that ultrafast, real-time, lable-free analysis of an individual DNA can be done by nanogap detector inside nanofluidic channel[21]. The detector uses a long nanfluidic channel to stretch a DNA strand into a linear chain, while using a nanogap detector, consisting of a pair of gold nanowires with a gap as small as 9 nm, to measure the electrical conduction perpendicular to the DNA backbone as it passes through the gap (Fig. 1e). A typical nanogap detector has a fluidic channel of 50 μm length, 45 nm width, and 45 nm depth, and a pair of metal nanowires of 45 nm width, 18 nm thickness, and different gap sizes and gap-heights that vary from 20 to 9 nm and from 30 to 16 nm, respectively. Using this device, electrical signals caused by 1.1 kilobase-pair (kbp) double-stranded (ds)-DNA passing through the gap can be observed. However, to improve the detection resolution of nanogap detectors toward single-base detection, as suggested by the authors, the nanogap dimensions, DNA flow speed across the channel and the fluctuations in DNA translocation time need to be optimized.

Gold nanoparticles-labeled biosensing

It is worth mentioning that a gold nanoparticle (Au NP) has been used as labels for ultrasensitive electronic detection[22]. The probe DNA is immobilized in a narrow gap between two electrodes. A target DNA is cohybridized to the probe on the electrode and to a signaling probe on Au NPs. Au NPs are used to bridge a nanogap, the target molecule is therefore detected by the observation of conductance change.

Fig. 2a presents the concept of electron transistor with using Au NP chain bridged a gap. Submonolayer gold colloidal particles of 10 nm diameter deposited on a SiO_2 substrate, by using an aminosilane as an adhesion agent, transform themselves into short chains of gold colloidal particles after a subsequent dithiol treatment and an additional gold colloidal particle deposition. These chains bridged a 30 nm gap formed between source and drain metal electrodes defined by electron beam lithography forming a one-dimensional current path consisting of three particles[23] (Fig. 2a1). The device exhibited a clear Coulomb staircase and a periodic oscillation of conductance as a function of gate voltage which corresponded to a three-dot (four-junction) multitunnel junction structure.

An alternative modulated strategy uses both molecular self-assembly and ac trapping of Au colloids to form a bridged gap device and to perform transport measurements of electronic molecules[24]. As two or more nanoparticles bridging the gap (Figure 2a2), the resistance of this type of Au electrode-nanoparticle assembly typically varies from
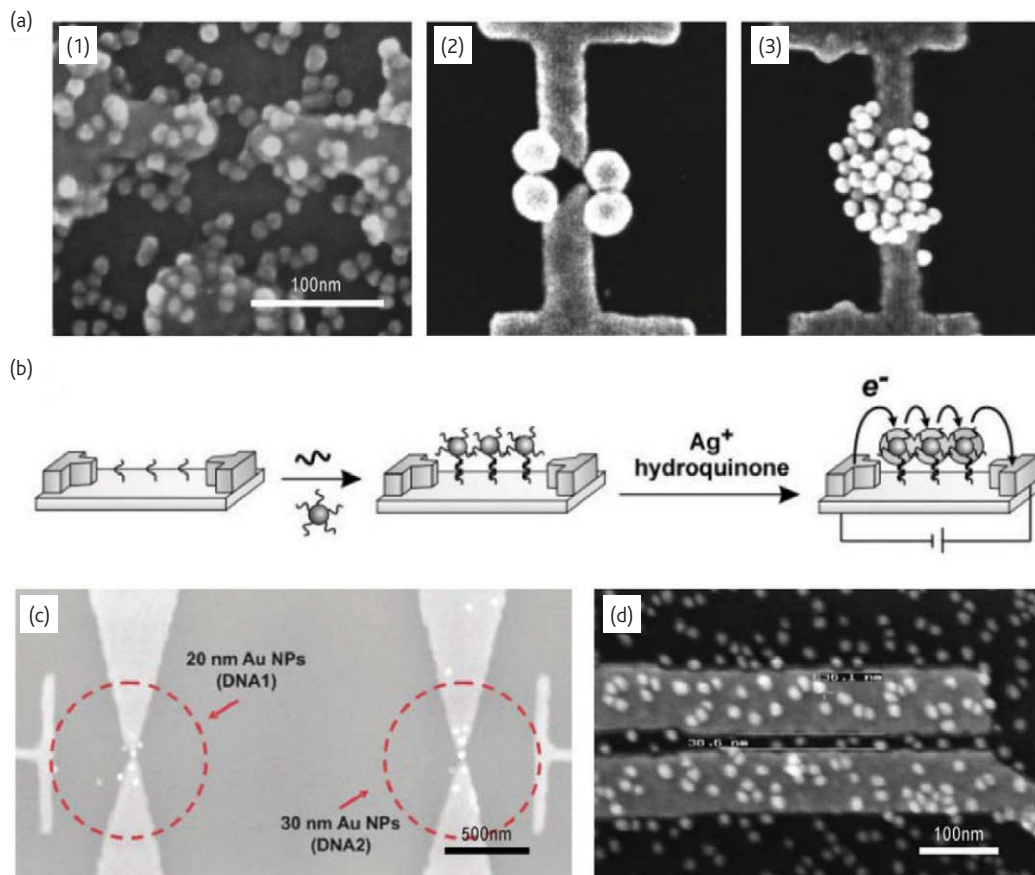
Fig. 2 Gold nanoparticles-labeled nanogap devices for biosensing. a) Concept of electron transistor using Au NP chain bridged a gap. (1) SEM observation of a three-dot gold colloidal particle chain incorporated in a system of source, drain, and gate metal electrodes[23]. (2) SEM image showing a few 120 nm Au NPs in a 40 nm gap[24]. (3) SEM image showing multiple 40 nm Au NPs clustered in and around a 60 nm gap[24]. b) Scheme showing concept behind electrical detection of DNA in which the binding of oligonucleotides functionalized with Au NPs and silver deposition leads to conductivity changes associated with target-probe binding events[25]. c) SEM image of single 20- and 30-nm-diameter Au NPs assembled from solution and bridging the nanogaps[26]. d) SEM image of the nanogap electrode after incubation of human serum and secondary anti-human antibodies-labelled gold nanoparticles(Ab^{ll}-Au NPs) with pA as probes[28].

100 kΩ to a few tens of MΩ. When the nanoparticle size is smaller than the gap, a larger number of particles cluster in the gap region. A typical value of resistance for such an assembly exceeds 100 MΩ (Fig. 2a3).

These works obviously provide a motivation for the electric detection of biomolecules using a labeled nanoparticle nanobridge.

A milestone discovery was by Mirkin and co-workers[25], who studied the use of metal nanoparticles, such as gold nanoparticles, as labels for sensitive electronic transduction of different biomolecular recognition events (Fig. 2b). After hybridization with target DNA and Au NPs labeled detection probes, Au NPs were localized into an insulative gap. The subsequent silver deposition to enlarge the gold NPs created a "conductive bridge" across the insulative gap terminated with two conductive electrodes. Using this method, target DNA can be detected at concentrations as low as 500 fM with a point mutation selectivity factor of ~100,000:1.

However, the synthesis of the nanoparticle labels requires a complicated and tedious process and is time-consuming. The need

of silver deposition for signal enhancement which increases the complexity of the detection process, and prevents the recycling of the chip, is possible by increasing the temperature above the melting temperature. Moreover, the non-target-related (nondiscriminative) deposition of silver onto electrodes itself and onto a silicon oxide background in the gap can significantly lift the background response and even lead to falsely positive signals. Finally, due to the large gap, a direct current was not detected: ligands within the gap were bound by receptors labeled with Au NPs and a significative conductance change was detected only after the application of a silver enhancer solution.

Several avenues have been proposed for addressing these limitations. One attractive approach relies on the dip-pen nanolithography (DPN) and DNA-directed assembly of nanoscale electrical circuits[26].

DPN is a nanofabrication tool that allows one to deposit molecules on a variety of surfaces with a coated atomic force microscope tip in a controlled fashion on the sub-100 nm to many micrometer length scale[27]. Therefore, the electrodes and the gaps between micro- and

nanoelectrodes can be functionalized with the desired DNA sequences by DPN, and the complementary DNA-functionalized nanoparticles can be selectively hybridized to such gap regions from solution. Fig. 2c shows single 20- and 30-nm-diameter Au NPs modified with DNA sequence 1 and sequence 2, which were deposited to bridge the gap of two adjacent electrodes. This emphases that the present approach allows us to assemble multiple, different nanostructures onto the same chip in a single chemical assembly step.

It is possible also to use a nanometer size gap (typically less than 100 nm between two planar electrodes) with a functionalized surface in the vicinity of the gap for the electrical detection of a biological interaction[28-30] (Fig. 2d). The local surface functionalization was designed to concentrate the ligand/receptor complex between the electrodes, i.e., to increase the sensitivity of the detection. The receptor was labeled with gold particles whose size was less than the size gap. In this case, two or three orders of magnitude of the conductance variation were observed without having to use a silver enhancer solution with biotin/streptavidin or biotin/antibiotin antibodies model biomolecular interactions. The concentration of the detected streptavidin or of the antibodies was in the range of a few 10^{-8} M.

Similarly, this method allows distinguishing probes to have different capture properties. For instance, immunoglobulin G (IgGs) in human serum can be detected using protein probes[28]. The detection is based on the capture of IgGs by a probe immobilized between gold nanoelectrodes of 30-90 nm spacing. The captured IgGs are further reacted with secondary antibodies labelled with Au NPs). Insertion of Au NPs into the nanogap resulted in an increase in conductance through the nanogap. Very recently, sub-2-nm nanogaps were fabricated via a novel electrical stressing approach[31]. The nanogaps exhibit substantial ionic-current reduction in near-physiological conditions. Although no data has been shown in the paper about DNA detection in aqueous solution by utilizing these nanogaps, the polymer-protected sub-2-nm nanogap holds great potential in the capture of molecules, peptides, or DNA, and detecting/studying these molecules in aqueous solution.

Even though some excellent results have been reached, however, coupled with the complex chemistry of labeling the probe or target analytes with biomolecules, the devices come with a healthy price tag and somewhat limited capabilities[32].

Nanoparticles-enhanced biosensing

The first issue that we should address in this part is that the role of nanoparticles is not for biomolecules labeling but for signal enhancement in ultrasensitive detection of biomolecules with a nanogapped biosensor. During the detection of nucleic acids, the number of specific DNA sequences in a sample might not be enough for precise detection. The most advanced solution to this problem is to use an additional step for sample preparation, such as polymerase chain reaction (PCR) or similar target-amplification techniques, to

amplify the DNA and reach the detection threshold. A major challenge is the development of methods that do not rely on polymerase chain reaction (PCR) or comparable target-amplification systems that require additional instrumentation and reagents that are not ideal for point-of-care or field use. One way to do this is to introduce conductive nanomaterials to enhance the signals.

Conductive nanomaterials enhanced nanogap biosnesors are desirable to overcome such limitations by virtue of their large-scale integrability, easy read-out and higher sensitivity. The sensing layer was prepared according to different methods, among which was self-assembly by chemical bonding. Generally, two different routes to conductive tag formation in the nanogap and their basic principles of amplification have been reported in the literature, and these are briefly described below.

Gold nanoparticles layer enhancement

Monolayer gold nanoparticle

Monolayer of Au NPs has been reported based on self-assembly onto the silicon dioxide surface within nanogap and proposed to function as a DNA sensor[33-35]. The presence of the Au NPs in the nanogap can reduce the distance by which electrons propagate between the DNA molecules.

The nanoparticles in the nanogap could act as hopping sites which amplify the conductance of hybridized DNA strands. It is found that the conductance is very low for either assembled Au NPs or Au NPs with single-stranded DNA. This observation is attributed to the poor conductance of single-stranded DNA. Electrons will localize to single-stranded DNA and cannot propagate through the DNA itself. However, the conductance (10^{-11} S) significantly increases with the hybridization of double-stranded DNA. Therefore, the electrical conductance for single-stranded DNA cannot be amplified by the preassembled Au NPs. In contrast, the electrical signal of doubled-stranded DNA can be amplified by the Au NPs. This observation clearly indicates that single-stranded DNA is not a good conductor, in contrast to double-stranded DNA[33].

This kind of DNA sensor provides a sensitive and label-free detection. For instance[35], with the help of 1 nM capture DNAs and the monolayer of gold nanoparticles within 72 nm gap, this sensor is able to analyze target DNA sequences at very low concentration of 1 fM.

Multilayer gold nanoparticle

Unfortunately, the current through the Au NPs monolayer is detectable at a magnitude of pA if the applied voltage is up to 1 V. And the *I-V* curve of monolayer gold nanoparticles (14 nm) does not obey Ohm's law in the range between -1 to 1 V at room temperature[36].

Chen, *et al.,* suggested a multilayer of Au NPs to be used as amplifier in biodetection[36-41] (Fig. 3a). Firstly, a self-assembly Au NP monolayer is immobilized in the gap by carbon strains after a nanogap is fabricated between two microelectrodes. Then, the single strand
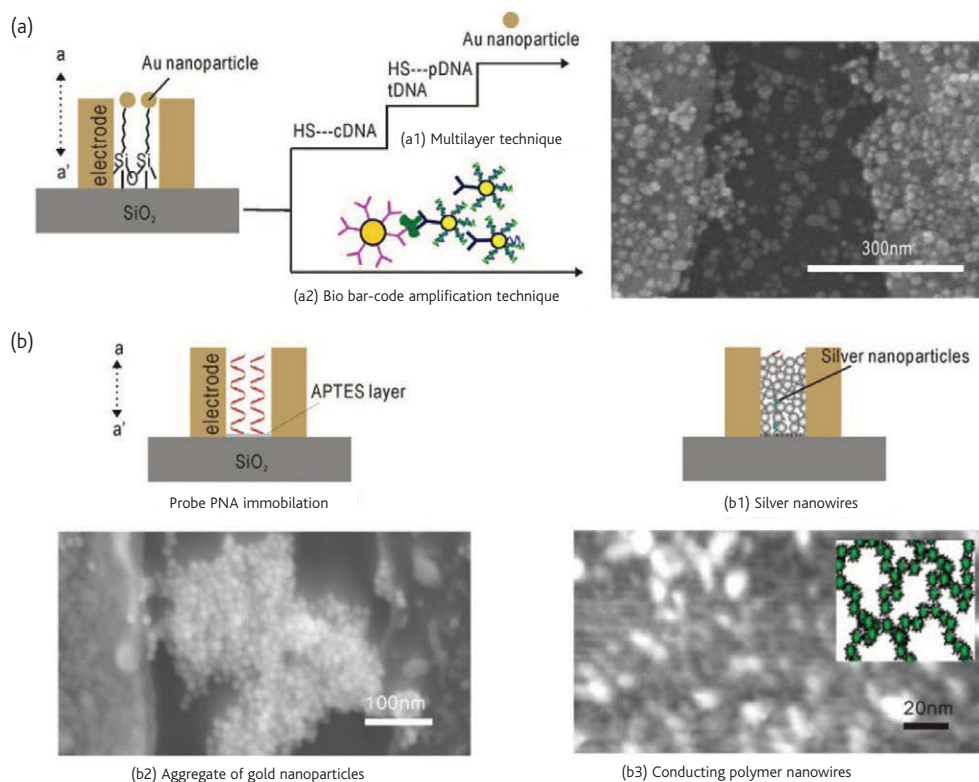
Fig. 3 Nanoparticle-enhanced nanogap devices for biosensing. a) Signal enhancement by gold nanoparticles. Before taking biomolecules detection, self-assembly monolayer of Au NPs is established on SiO$_2$ surface between nanogaps. (a1) Example of signal enhancement by multilayer of Au NPs[36,37]. (a2) Signal enhancement by combining of multilayer of Au NPs and bio-barcode amplification technique[42,43]. The picture is a typical FE-SEM image of the Au NPs multilayer with bio-barcode DNA amplification for target HCV antigen concentrations at 100 fg/μL for the first specific binding between 2B2, GP, and HCV antigen[43]. b) Conducting nanomaterials are introduced into nanogap after biomolecules immobilization. (b1) Silver nanowire resulted in ultrasensitive detection of nucleic acids[44]. (b2) Aggregate of gold nanoparticles (ANPs) as a conductive tag for electrical detection of oligonucleotide. The picture shows that the gap was bridged by ANPs[45]. (b3) Conducting polyanline nanowires in nanogaps for microRNAs detection. The image shows the stage after hybridization and polyaniline nanowire deposition[46].

thiol-modified capture oligonucleotides (labeled as cDNA) is added to the nanogap and immobilized onto the surface of monolayer Au NPs. Selective binding occurs among immobilized capture oligonucleotide strand, suspended probe oligonucleotide (labeled as pDNA), and target oligonucleotide strand (labeled as tDNA) in the sample solution. One end of the probe oligonucleotide DNA is modified by thiol. Finally, the measured spot is rinsed with a PBS solution before adding gold nanoparticles. Strictly, the final stage of multilayer gold nanoparticles follows a "sandwich" structure.

A further method was also suggested to fabricate multilayer gold nanoparticles[36]. A monoclonal antibody is immobilized on the top surface of the first layer of Au NPs (14 nm). The second layer of Au NPs is formed through specific binding among a target antigen [hepatitis C virus, (HCV)], the monoclonal antibody, and the conjugate of an Au NP-polyclonal antibody. The measured I-V curve over the multilayer gold nanoparticles depends on the concentration of the HCV antigen. The detected current of the multilayer Au NPs is up to 0.8 mA for an applied gate voltage of 1V at the HCV antigen concentration of 100 ng/mL.

On the basis of self-assembled multilayer Au NPs, they introduce magnetic nanoparticle probes functionalized with bio-barcode receptors to detect low concentrations of target HCV antigen[42,43]. Magnetic nanoparticles and bio-bar-code DNA are used to amplify obtainable current through nanogap electrodes from the extremely low concentration of target DNA. In this way, the method is easily sensitive enough (a sensitivity of up to 1 pg/μL) to detect as low as 1 fM DNA molecules.

In situ formation of conductive nanomaterials
Conductive nanomaterials can be also linked after hybridization. For example[44], peptide nucleic acid (PNA) probes were immobilized in the gaps of a pair of finger microelectrodes and they were then hybridized with their complementary target DNA. After this, pectin molecules were introduced into the DNA strand via zirconium-phosphate and zirconium-carbonate chemistries, and these were oxidized by periodate in acetate buffer (pH 3.98). The newly produced aldedyde groups act as a reactant to reduce ammoniacal silver ion and produce silver nanoparticles, which bridged the gap of

the interdigitated microelectrode (Fig. 3b1). The conductance of the metallic nanoparticles correlated directly with the amount of the hybridized DNA. Using this polysaccharide templated silver nanowire, a much higher sensitivity was achieved at 3 femtomolar (S/N > 3) under optimal conditions. It was observed that cDNA can be detected within a dynamic range of 1.0 fM to 10.0 pM (4 orders of magnitude) with the regression coefficient R as 0.99.

An aggregate of gold nanoparticles (ANPs) also can be used as a conductive tag to bridge the nanogap electrodes for electrical detection of oligonucleotide[45] (Fig. 3b2). 22-mer oligonucleotide DNA at low concentration, from 50 fM to 10pM, can be detected. Fig. 3b2 presents the SEM picture of modified gap with as-prepared aggregate of nanoparticles.

Even though Au NPs have exhibited excellent behavior for sensitive electronic transduction of different biomolecular recognition events, the gold nanoparticle-based assays have rather limited applications in microRNA (miRNA) analysis because of the inability for much smaller gold nanoparticle-detection probe conjugates to bind with such small miRNA templates. The extremely small size and similarity among family members of miRNAs have presented challenges for developing ultrasensitive miRNA assays. To eliminate the second hybridization process with the Au NP-detection probe conjugates, one possible approach would be a highly specific one-step *in situ* amplification process, in which the amplifier is directly associated to the target nucleic acid, and miRNA in particular. For example[46], the position of conductive polyaniline (PAn) nanowires were carried out by an enzymatically catalyzed method, where the electrostatic interaction between anionic phosphate groups in miRNA and cationic aniline molecules is exploited to guide the formation of the PAn nanowires onto the hybridized target miRNA (Fig. 3b3). The conductance of the deposited PAn nanowires correlates directly to the amount of the hybridized miRNA. Under optimized conditions, the target miRNA can be quantified in a range from 10 fM to 20 pM with a detection limit of 5.0 fM. In principle, a much lower detection limit could be realized when working with longer target nucleic acids because the bridging of the nanogaps by the PAn nanowires can be realized with fewer long nucleic acid molecules.

Obviously, these methods directly utilized chemical ligation and amplification for signal read-out and thus eliminated the use of labeling probes, which greatly simplifies the detection procedure (the synthesis of the NP labels requires a complicated and tedious process and is time-consuming.). Multiplex detection can be easily realized by introducing different capture probes onto the biosensor array, which will make it more versatile for various research purposes.

Nanogapped gold particle film for biosensing

This technique provides an opportunity to realize label-free DNA electronic sensing on a chip. The approach relies on the dithiol molecule which functions as both the linker between the gold

nanoparticles and the spacer for producing the tunneling barrier, the energy of which changes upon hybridization occurring between the particles.

Gold nanoparticles were adsorbed into both the glass and Pt electrode, and bridge molecules (decanedithiol) were used to make a gap between each particle[47-52] (Fig. 4a). After modification with thiolated DNA, DNA molecules can be detected by monitoring the resistance changes. For instance[49], upon sample addition, a resistance decrease was immediately observed with S/N ratios above 40, followed by a steady state within 2 min (Fig. 4b). The magnitude of the response depended on the number of the mismatched base pair (bp) in DNA, and the largest among the samples was the complementary strand (0.19 Ω). An increasing number of mismatches led to a decrease in the magnitude, and the 11-bp mismatched DNA showed the smallest response (0.05Ω). It should be noted here that the resistance change behaved in a nonlinear fashion with respect to the number of mismatches. The behavior can amplify the presence of a 1-bp mismatch and be characterized as an important diagnostic advantage on detecting single nucleotide polymorphism.

Generally, using this approach, a nanogapped molecular electronic device with an electrode spacing accuracy of a few nanometers can be fabricated. The gap between adjacent nanoparticles created with 1,10-decanedithiol is estimated to be ca. 1.3 nm, and the electrode separation can be as large as in the micrometer scale when the dithiol-linked nanoparticles are deposited over the chip as a film. The fabricated nanogaps in this system can be equal to or slightly less than the length of the molecule of interest. This technique might provide an additional method to overcome the resolution limitation (order of ~10nm) of the current lithographic technique and make the construction of high-density electrical DNA array devices become possible.

According to a previous report, Au NPs separated by a 1.3-nm gap could be used for recognizing the hybridization event; however, the concentration range was limited (detection limit of ~25 pmol) because not every probe could hybridize with a target DNA strand in the gap between the particles[48,49,51]. Thus, they were not completely responsible for the formation of the conducting path on the surfaces of respective Au NPs.

Nanogapped gold particle film has been developed into an open bridge-structured gold nanoparticle array for label-free DNA detection consisting of 46-nm parent and 12-nm son gold nanoparticles by hybridization[53].

A gap between adjacent 46-nm AuNPs fixed on the microelectrode due to less immersion times in the thiol binder solution, and the dispersion was larger than that of the previous report (~1.3 nm). To anchor the DNA-modified probe particles to the scaffold, a 1:1 colloidal mixture of probes A and B was applied onto the microelectrode after immersion into the ethanolic 1,10-decanedithiol solution (d). The SEM image of the array for several widths revealed that most of the probe
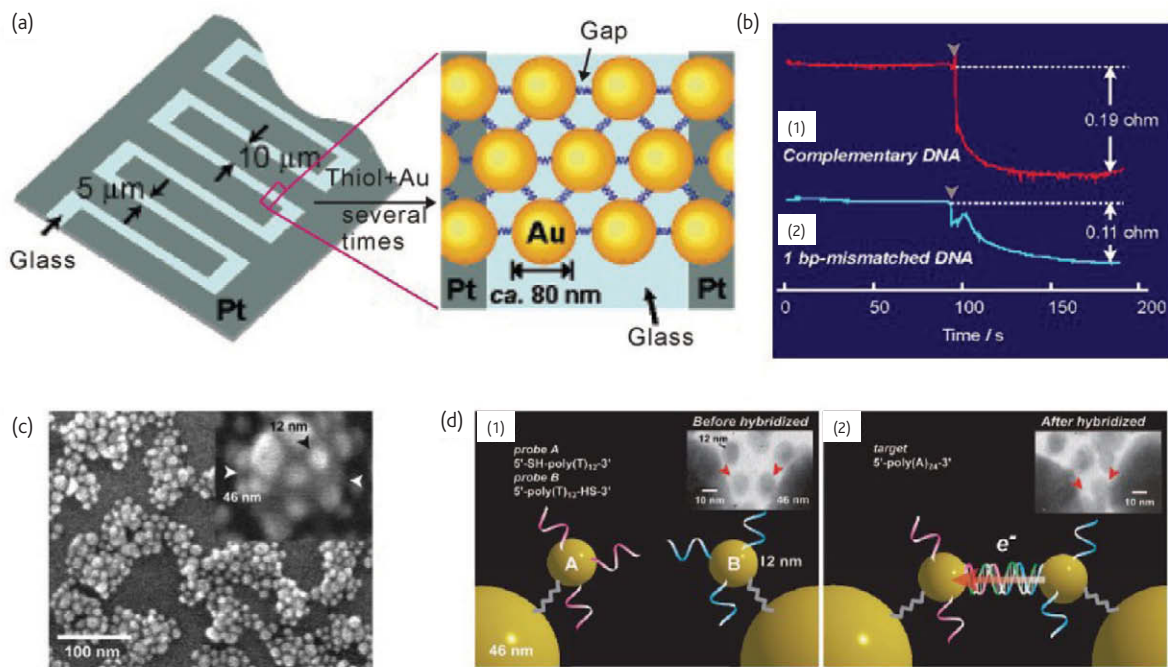
Fig. 4 Nanogapped gold particle film for biosensing. a) (Left) Illustration of interdigital electrode. (Right) Bird's-eye-view sketch of nanogapped gold nanoparticle film[49]. b) Resistance changes by hybridization of the probe with (1) complementary oligonucleotide (3'-AGA GTT GAG CAT-5') and (2) 1-base (3'-AGA GTT GAG CCT-5') mismatched sample strands[49]. c) SEM image of DNA-capped 12-nm Au NP probes modified 46-nm parent Au NP[53]. d) Conceptual illustrations of the array consisting of the DNA-capped 12-nm Au NP probes, A and B, immobilized on the parent 46-nm Au NP with dithiol: Probe configuration (1) before and (2) after the addition of 24-mer target. The inset is a TEM image of the Au NP array revealing around 46-nm particles[53].

particles (12-nm son gold nanoparticles) bind to the hemisphere of the parent surface (46-nm parent nanoparticles) as shown in Fig. 4c (average, 16 probes/parent). Even in a simple measuring method, a rapid response to the cDNA with a high S/N ratio of 30 over a wide concentration range and a detection limit of 5.0 fmol can be obtained. This is mainly because of not only the molecular conductivity of DNA[48,49,51], but also the shrinkage of the structural distance of the 12-nm probes in the gap of the 46-nm parent particles due to the hybridization (Fig. 4d).

Carbon nanotube nanogap devices for biosensing

Electronic devices based on carbon nanotubes (CNTs) are among the candidates to eventually replace silicon-based devices for biomolecular sensing applications[54]. However, one of the greatest challenges in CNTs molecular electronics is the ill-defined bonding between molecules and metal electrodes[55]. To eliminate this drawback, CNT-based FET (field-effect transistor) sensors can be replaced by such an improved strategy, in which a cut SWCNT with a sub-10 nm gap to be used as source (S) and drain (D) electrodes of a molecular electronics[55-63]. The target molecule is covalently immobilized in a narrow gap between carbon nanotube electrodes. After this insertion, the electric conductance across the electrodes increased, thus revealing the presence of the target. All of the elements in the resulting molecular circuits are naturally at small dimensions because the SWCNTs are one-dimensional conductors or semiconductors that are intrinsically the same size as the molecules being probed[55].

Fig. 5a shows the general concept of carbon nanotube nanogap biosensors. Briefly Au (50 nm) on Cr (5 nm) leads, (which are separated by 20 μm) form the source and drain contacts to an individual single-walled carbon nanotube. The tubes are then oxidatively cut by using ultrafine e-beam lithography and precise oxygen plasma that produces the nanogaps of 1-10 nm on the nanotube ends. The nanogap devices were electrically tested using the metal pads as source (S) and drain (D) contacts and the silicon substrate as a back gate (G)[57,58,60].

Fig. 5b shows an AFM image of one nanogap. By taking the imaging convolution of the AFM tip size into account, we can estimate that an upper boundary on the size of a typical gap in these micrographs is ~10 nm[55].

During DNA electrical measurements, two different methods could be used to bridge these gaps[57]. One is that one end each of the two strands of the DNA duplex is bound to the SWCNT electrodes (Fig. 5c). The other is that a single strand is bound between the ends of the SWNT electrodes (not shown). Well-matched duplex DNA in the gap between the electrodes exhibits a resistance on the order of 1 MΩ. A single GT or CA mismatches in a DNA 15-mer increases the resistance of the duplex ~300-fold relative to a well-matched one.

The most important issue of CNT nanogap device is the formation of a covalent bond between each terminus of a DNA molecule and
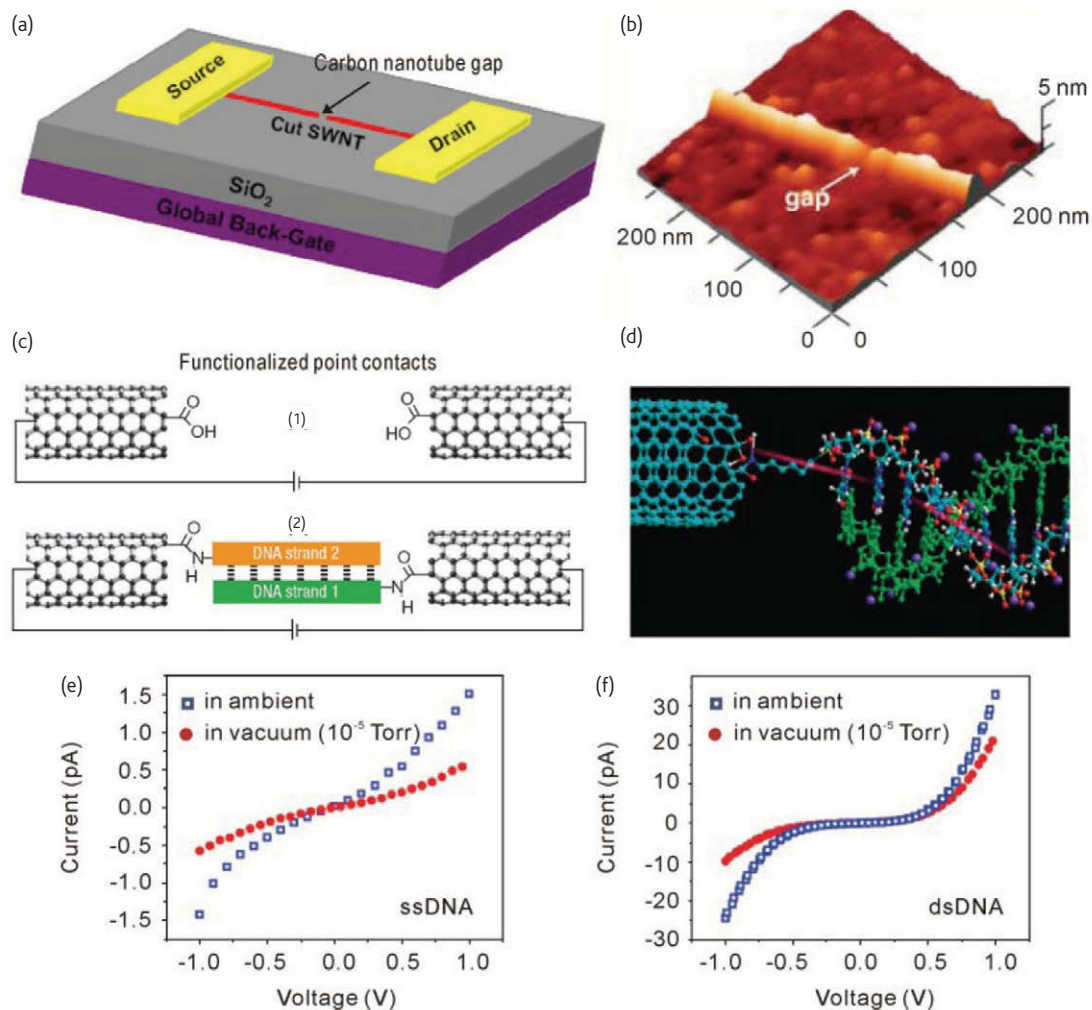
Fig. 5 Carbon nanotube nanogap devices for biosensing. (a) A cut metallic SWCNT transistor connected by large metal leads as the S/D electrodes and the silicon wafer as the global back-gate[57]. (b) AFM image of the carbon nanotube nanogap[55]. (c) Illustration of sensing mechanism of carbon nanotube nanogap[57]. (1) Functionalized point contacts made through the precise cutting of a SWCNT with oxygen plasma. (2) Example of bridging by functionalization of both strands with amine functionality. (d) Molecular diagram highlighting the covalent bonding between an amine-terminated ssDNA and a carboxyl-functionalized SWCNT nanoelectrode via a ($-CH_2-$)$_6$ spacer. Charge transport takes place through the stacked base pairs in a helical duplex[63]. (e) and (f) Current flow at room temperature through single ssDNA and dsDNA molecules, respectively, in ambient and in vacuum conditions[63].

the functionalized end of a SWCNT electrode. Establishment of a strong electronic coupling between the trapped molecule and the nanoelectrodes facilitates the charge transport through the system without the Coulomb blockade effect[63] (Fig. 5d). The covalent attachment to molecules at functionalized point contacts through amide linkages avoids the limitation of the poorly defined nature of the contact between the molecules and metal surface, and one of the serious drawbacks of thiol chemistry, the oxidative oligomerization of dithiols. The amine-attachment chemistry is well developed in peptide synthesis, and the amide bonds that are formed are extremely stable.

DNA-substrate interactions have been known to be critical in determining the conductivity of an immobilized molecule. The strong interaction between DNA and a silicon oxide surface induces a large compression of the deposited DNA[64,65]. According to this, in Choi's work, the bridging DNA molecule suspends over a trench without touching the silicon dioxide surface[63]. The presence of a nanotrench, between the SWCNT electrodes, that eliminates the contribution of the oxide surface to the charge transport through a DNA molecule. The suspended DNA molecule in the present system mitigates the problem of compression induced perturbation of charge transport.

Statistically, for the majority of the devices, a current value in the range of 25-40 pA when a dsDNA molecule bridged the SWCNT electrodes was observed. In comparison, an ssDNA molecule carries a much lower current (~1 pA, or less), primarily due to the lack of regular stacking of the nucleotide bases. Application of the back-gate voltage
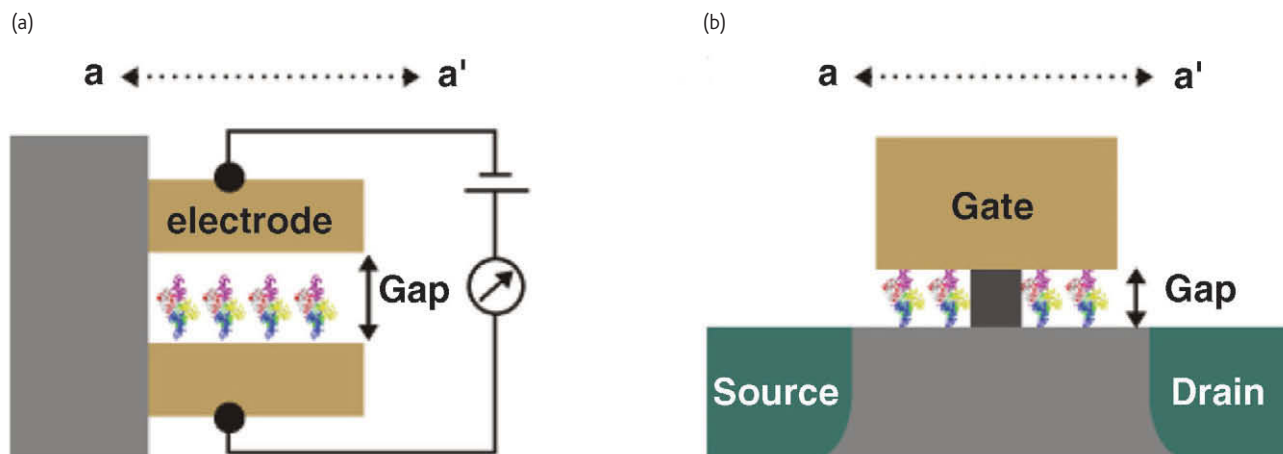
(a)

(b)

Fig. 6 Vertical nanogap. Schematic of a FET device with a vertical nanogap for biomolecule sensing. a-a' direction of the dotted line shows the filled nanogap by biomolecules. (a) Two terminals. (b) Three terminals

revealed that the bridging DNA molecule forms a p-type semiconducting channel between the SWCNT electrodes[63] (Fig. 5e and f).

Vertical nanogap devices for biosensing

In the design of vertical nanogap, both electrodes are vertically situated in perpendicular direction. Such nanogap devices can be classified into two groups: two-terminal and three-terminal nanogaps, as illustrated in Fig. 6. The detailed information is discussed below:

Nanogap device with two terminals

Although the dielectric properties of DNA solution have been widely investigated, early approaches were limited at low frequency by the parasitic noise due to the electrical double layer impedance[66]. Nanogap has the potential to serve as a biomolecular junction because its size (5-100 nm) minimizes the electrode polarization effects regardless of frequency. Lee and co-workers produced a nanogap biosensor consisting of a heavily doped single crystal silicon electrode and a polysilicon electrode vertically separated by a fixed distance of 20-300 nm (defined by a small silicon dioxide spacer)[66-70] (Fig. 7a). Biomolecules bound to a gap surface can be detected by measuring dielectric properties. In their sensing model, they proposed that, at an electrode surface in an ionic solution the association of ions from solution to the oppositely charged electrode surface follows the Poisson-Boltzmann equation. By decreasing the potential drop across the double layer one can effectively decrease the capacitance - this occurs when two double layers overlap. Therefore, the double layer capacitance can be reduced by decreasing the gap size between electrodes to the nanometer scale (60-100 nm).

A proof of concept was demonstrated by immunosensing the glycoprotein laminin, which is clinically relevant to kidney disease at a concentration of 0.5 μg/ml. Dissipation factor measurements for different laminin concentrations indicated a detection limit of

10 ng/ml in a 30 μl droplet[69]. In another work[68], they showed low frequency dielectric measurements of protein structural transitions in aqueous solution using a nanogap biosensor. Ionic strength effects on low frequency measurements were lessened when using a nanoscale dielectric cell, and decreased along with electrode gap size. Measurements in nanogap sensors between 10 kHz and 1 MHz were found to be especially insensitive to ionic strength fluctuations. The alkaline structural transition of Cytochrome c was successfully monitored using dielectric spectroscopy.

Water structure is a very powerful topic, and studying how water behaves within nanoscale structures is fundamental in understanding the role of water in biology. Protein folding, DNA hybridization, and enzyme substrate interactions are just a few areas where the structure and position of water is paramount. Without water, there would be no cell membranes, no ion transport, and no protein ligand interaction. Lee *et al.,* continuously studied the changes in the structure of water and ice using a nanogap biosensor[70]. The structural changes in a network of H_2O (water or ice) molecules were observed. Using a 20 nm polysilicon gap, 20-mer single stranded DNA (ssDNA) oligonucleotides in 100nM 1.2 pl aqueous solutions was detected.

Impedance detection was often employed to detect biomolecules. The principle is based on electrical impedance changes measured at a particular frequency due to changes of the effective dielectric constant after biomolecules specific binding within the nanogaps between two electrodes. For example, nanogap-impedance biosensors with electrode separations of 75 nm have been fabricated by means of standard optical lithography and a sacrificial layer technique. Due to a large surface-to-volume ratio and high sensitivity, these sensors are superior in comparison to open interdigitated electrode structures[71] (Fig. 7b). As a model, the blood coagulation factor thrombin was detected. As specific receptors, either an antibody or a RNA-aptamer has been used[72]. By using the 75 nm gap-structure it is also possible to discriminate between the unspecific
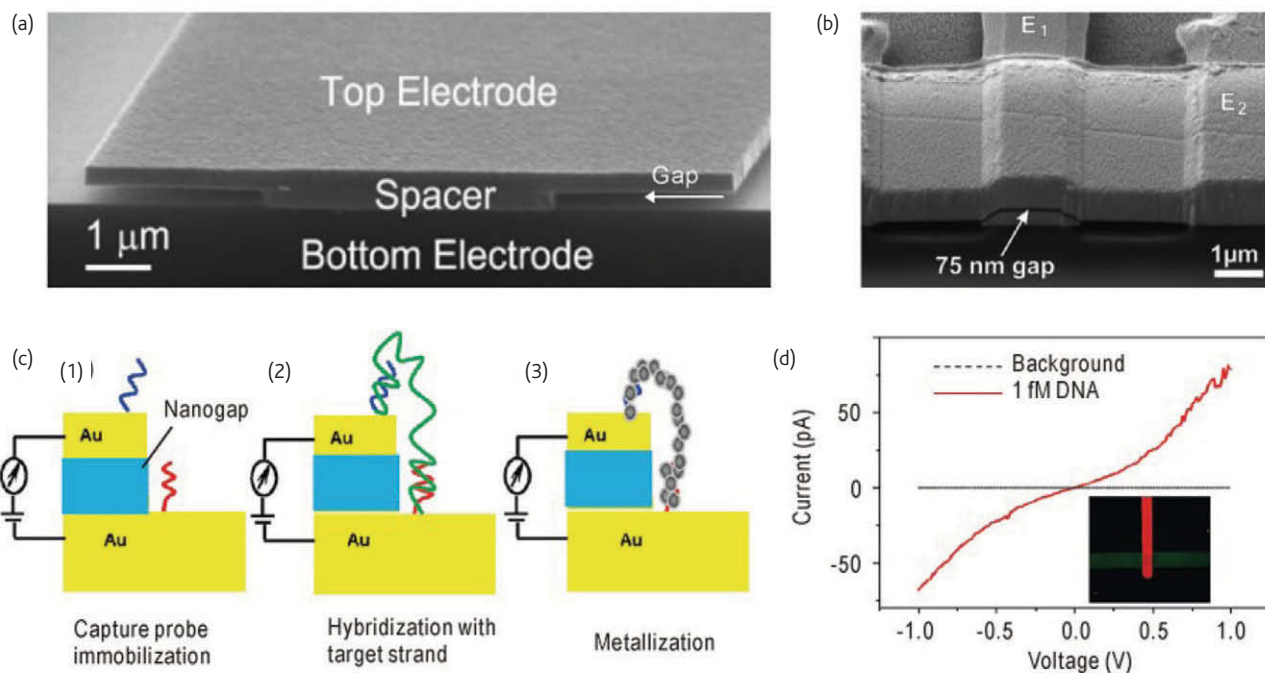
Fig. 7 Vertical nanogap device with two terminals. a) A nanogap biosensor consists of a heavily doped single crystal silicon electrode and a polysilicon electrode vertically separated by a fixed distance of 20-300 nm, defined by a small silicon dioxide spacer[67]. b) A nanogap-impedance biosensor. E1: bottom Au electrode; E2: top Au electrode[73]. c) Sensing procedure based on the electronic transduction mechanism of nanoMIM[12]. (1) two different capture probes immobilization across the nanogap; (2) hybridization with target DNA; (3) formation of silver wires along the backbone of the bridging molecule that results in formation of an electrical conducting pathway(s) between the electrode pair. d) Representative I-V curve for 1.0 fM target DNA as referred to background. The inset shows fluorescence image after immobilization of CP2 and hybridization with respective complementary DNAs tagged with Cy3 and FAM dyes on the two electrodes separated by a nanogap[12].

binding of lysozyme and the specific binding of the Rev peptide to the Rev aptamer. The higher sensitivity was found to be 1.3% for the nanogap device, while a value of only 0.3% was determined for the IDC-sensor[73].

A major advantage of impedance biosensors is that they do not require labels which are complicated to prepare and can interfere with the biochemical reaction itself[74]. Furthermore, impedance biosensors allow a real-time monitoring of the sensor-signal and give therefore rise to kinetic aspects of the ligand-analyte interaction. The nanogap structure significantly reduces electronic noise, while having an increased sensitivity based on their low internal volume.

Most nanogap biosensors usually follow the protocol of "filling the gap"[75]. Gao and co-workers reported an attractive alternative nanogap device (or call it nano metal/insulator/metal multilayer (nanoMIM)) for detecting DNA sequences[12]. In this case, two electrodes were separated by an insulating gap. A nanometer-thick layer of SiO_2 (insulator) was sandwiched between a pair of vertically stacked metal layers (conductors). The SiO_2 insulating layer forms a "nanogap" between the top and the bottom metal electrodes on which two capture probes with different sequences, complementary to the two termini of the target DNA, respectively, were immobilized. Bridging of this nanogap by the target DNA strand, upon hybridization and subsequent silver nanowire formation, creates a primary current pathway (Fig. 7c). Noncomplementary DNA strands, (which fail to hybridize with the capture probes) do not bridge across the insulator layer and thus will not contribute to the current between the two metal electrodes.

The sensing mechanism relies on bridging the nanogap upon hybridization of the two termini of a target DNA with two different surfacebound capture probes, followed by a simple metallization step. Using this device, about 2 orders of magnitude enhancement in conductance, as referred to a clean background (<1.0 pS) observed at a control sensor, was obtained in the presence of as little as 1.0 fM target DNA (Fig. 7d). A linear relationship between the conductance and the DNA concentration was obtained from 1.0 fM to 1.0 pM with an exceptional signal intensity of 2.1×10^4% change per unit concentration.

The inset in Fig. 7d provides an excellent visual proof that two different capture probes were very selectively immobilized on the surfaces of a pair of nanometer-spaced electrodes. The fluorescence image strongly suggests a high surface coverage of the immobilized capture probes and an excellent hybridization efficiency, which paves the way for the development of ultrasensitive DNA sensing devices. This new sensor offers "a scalable and viable alternative for DNA testing" and "holds significant promise for the detection and diagnosis for debilitating diseases such as cancer, cardiovascular problems and infectious viruses".

Most recently, a novel signal-amplification scheme for detection of DNA involving gold nanoparticles labeled biosensor with a vertical nanogap was reported[76]. The gap is about 20 nm. The target is an
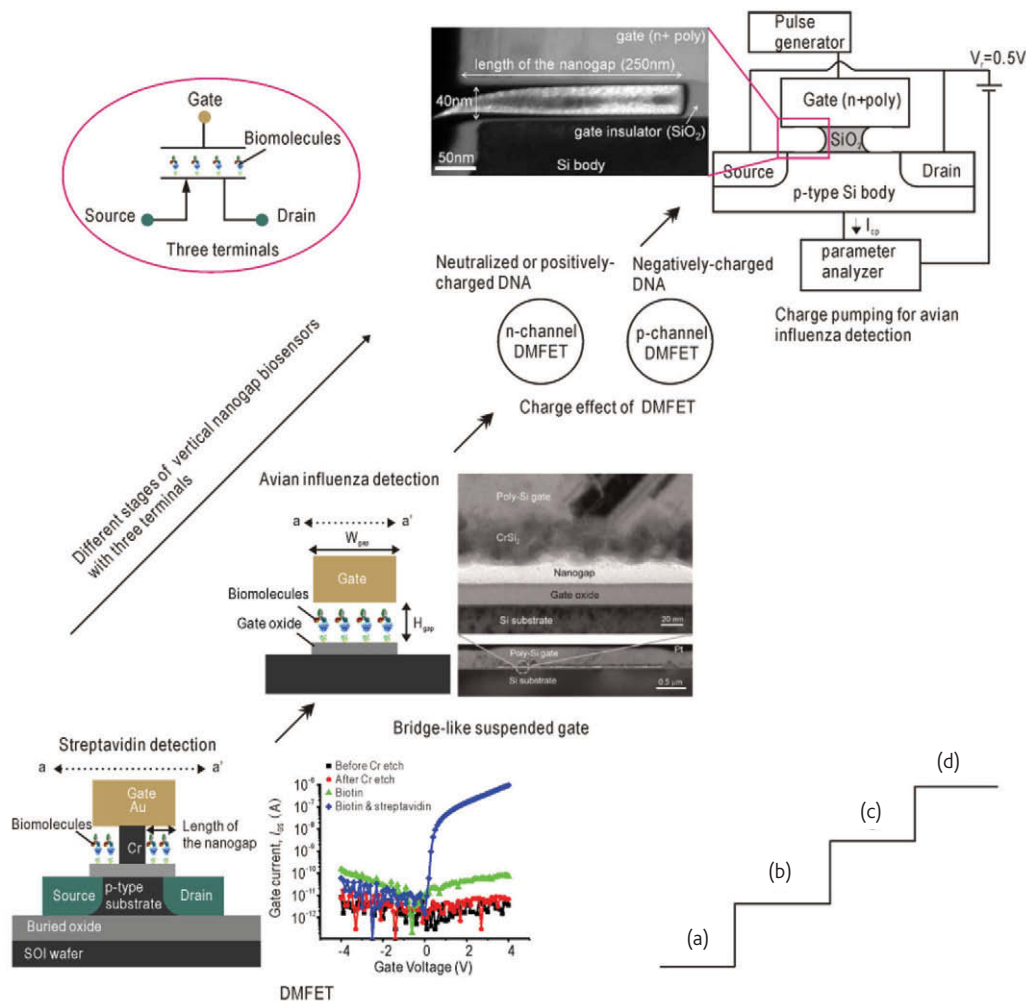
Fig. 8 Vertical nanogap device with three terminals. (a) (Left) A cross-section of the nanogap DMFET device for electrical detection of biotin and streptavidin based on dielectric constant effect. (Right) I_{GS}-V_{GS} characteristics of the nanogap DMFET device before and after biotin-streptavidin biomolecules are immobilized in the nanogap at V_{DS} =0.05 V[77]. (b) (Left) A cross section of the nanogap FET with bridege-like suspended gate for electrical detection of avian influenza. (Right) TEM image of the nanogap FET with a nanogap of 20nm in height[80]. (c) Studies of charged-DNA detection based on charge effect in the nanogap DMFET device[81]. (d) A charge pumping method for avian influenza detection in the nanogap FET[83]. The inset shows that the mechanism of nanogap FET biosensors: when biomolecules are introduced into the nanogap, they increase the gate capacitance relative to the air gap, and a threshold voltage, V_T, shifts in the negative direction. Thus, by monitoring the change in V_T, it is possible to detect the specific binding of biomolecules.

oligonucleotide conjugated to gold nanoparticles, whereas the probe is an oligonucleotide immobilized on nanoelectrodes. As a consequence of a target-probe binding event, a conductive bridge forms between the electrodes[24], resulting in a discrete change of the electrical conductivity with single biorecognition event sensitivity. The main improvement of this approach is that the smaller size of the inter-electrode gap (a few nanometers) makes single-event sensitivity possible and multiple layers of self-assembled gold nanoparticles for signal amplification between electrodes unnecessary.

Nanogap device with three terminals

In a typical FET device, electric current flows between the source and drain electrodes when the voltage applied to the gate exceeds a threshold voltage (V_T). V_T is determined primarily by the gate

capacitance between the gate electrode and the channel, and hence one can modulate V_T by changing the dielectric material of the gate. When biomolecules are introduced into the nanogap, they increase the gate capacitance relative to the air gap, and V_T shifts in the negative direction. Thus, by monitoring the change in V_T, it is possible to detect the specific binding of streptavidin to biotin[77].

On the basis of this mechanism, Choi and co-workers suggested that a dielectric-modulated field-effect transistor (DMFET) for biosensing based on change in dielectric constant caused by the introduction of biomolecules in a nanogap located at the edge of the gate dielectric in the DMFET[77] (Fig. 8a). A typical electrical characteristic of the DMFET nanogap shows that, before immobilizing the streptavidin, the gate leakage current is in the range of picoamperes, but it increases dramatically to microamperes after biotin-streptavidin binding due to

the intermolecular attractions (Fig. 8a, right, 300 nM of streptavidin in PBST, 0.01 M phosphate-buffered saline(PBS) + Tween20 0.05%, and about 3mM of biotin). It is believed that this is because the bound molecules provide a current path for electrons to flow to the gate. Compared with the detected limit and V_T change of ISFET[78] (100mM; 78mV) and EGFET[79] (1.5mM; 0.3V), the vertical nanogap DMFET device provides a sufficient level of sensitivity, V_T shifts dramatically by -0.73 V after the streptavidin (300nM) binds to the biotin layer in the nanogap.

The novelty of the DMFET nanogap device is its vertical configuration, which provides more design flexibility than the common horizontal configuration, which is usually fabricated by lithographic patterning techniques[75]. In case of DMFET, the fabrication process is based on one of conventional CMOS fabrication process. A few nanometer size of gap can be defined using thin layer deposition and wet etching process, which do not suffer from the lithographic resolution limit. The DMFET can show the dielectric property by capacitance measurement and I-V characteristics as well. In this situation, contact resistance is not important to change the threshold voltage. It can provide further degrees of freedom to design nanogap structure and to choose material for each corresponding bio-molecules. Furthermore, DMFET shows similar structure and electrical characteristics to those which conventional field effect transistors have. It makes it easier than two terminal nanogap devices to detect dielectric property of biomolecules by combination with read-out circuitry.

However, the flexibility of these devices in detecting other biomolecules or an unknown mixture of biomolecules remains to be evaluated. The main challenge will likely be calibrating the device so that a specific biomolecule can be identified with respect to the shift in the threshold voltage and the width of the nanogap. Nanogap DMFET poses another fundamental problem in that it is difficult to force a "solution" containing the biomolecular species to be detected into the small size of the nanogap (15 nm). The appropriate fluid dynamics in this case involves extremely low Reynold's numbers (in the range of 10^{-8}-10^{-6}). It is not clear if there will be adequate "mixing" of the solution necessary for this application.

To address this problem, a nanogap FET device with a suspended chromium gate has been developed[80]. A silicon dioxide (SiO_2) layer of 20 nm in height was grown on the active area of a p-type silicon wafer to form the gate oxide after source/drain formation and channel implantation (Fig. 8b). A suspended chromium gate of 40 nm in height was deposited and patterned. A distinctive feature of this nanogap FET is its bridge-like suspended gate, which allows biomolecules to move freely in and out of the nanogap channel beneath it. This kind of nanogap FET device developed as an efficient label-free electrical biosensor and used to detect AI using a specifically designed protein, SBP-AIa, which has silica-binding specificity.

The aforementioned DMFET, based on change in dielectric constant, has shown high sensitivity to biotin-streptavidin-specific binding, which was known to be nearly neutralized. However, in nature, there are

many biomolecules that show charged behaviors; DNA is one of the most important of these biomolecules, as it is known be the largest negatively-charged molecule[32]. When charged biomolecules such as DNA are introduced into the nanogap of a DMFET, its operation can be affected by this charge effect despite the known dielectric constant effect. To achieve the best possible performance of nanogap DMFET device towards different types of biomolecules it is necessary to study their charge effect of DMFET during electrical measurements. Choi's group demonstrated that the n-channel DMFET can preferably detect neutralized or positively-charged biomolecules. In contrast, a p-channel DMFET is attractive for improvements to the detection sensitivity of negatively-charged biomolecules[81] (Fig. 8c).

In practice, FET biosensors have many useful device parameters in addition to V_T. Hence, each device parameter can be utilized as a sensing parameter for detecting biomolecules. One possible device parameter utilized as a sensing parameter is the average density of the interface trap (D_{it}). The interface traps are located between a silicon channel and a gate insulator interface. They represent a very sensitive parameter that can affect the device characteristics. An extraction method related to this parameter – "charge pumping" - was developed in the 1990s[82]. Charge pumping provides information related to the distribution of traps, the energy level of traps, and the amount of trapped charge and the value of D_{it}. Due to the immobilized biomolecules in the nanogap, the interface property of the silicon channel is changed, giving rise to a modulation of D_{it}. Therefore, targeted biomolecules can be electrically detected by charge pumping[83] (Fig. 8d).

Conclusions

Different strategies used to develop electrical nanogap devices for biosensing have been reported in this review. Each method has its own individual advantages and disadvantages and very few offer both the promise of nanoscopic gap-size control and the likelihood of inexpensive and efficient fabrication. In many cases, they also do not cover the entire spectrum of the biosensing needs. Referring to the literature, field-effect (FET), resistive (impedance detection), and capacitive (dielectric detection) devices have been investigated more widely, using various nanogap biosensing devices. Nanoscience and nanotechnology including nanomanufacture and surface modification have taken a leading role in the realization of ultra-sensitive and highly selective detection of biological molecules.

A major goal is the efficient detection of molecular binding events of very small quantities of biomolecules, such as the binding (hybridization) between two strands of DNA. Many other kinds of molecules, including antibodies, enzymes or proteins, can be identified by specific binding

reactions. But when there are many different events occurring in a single sample, distinguishing between them becomes crucial. Combination with advanced nanotechnology such as dip-pen nanolithography or barcoded molecules not only offers another label-free alternative for biosensing, but the scale at which this method can be performed means there is the potential to produce chips that are the same size as microarrays, but with a major increase in the pattern density, leading to significant benefits in sensitivity. Finally, the 'lab-on-a-chip' community is constantly progressing towards the development of fully electronic multifunctional devices that can channel fluids and sort and detect cells or biomolecules[75]. As with most solid state biosensors, it will be a challenge to integrate the nanogap device with micro- and nanofluidic components for fluid handling and biomolecule delivery. `mt`

Acknowledgements

REFERENCES

1. Drummond, T. G., *et al.*, *Nat Biotechnol* (2003) **21** (10), 1192.
2. Bakker, E., *Anal Chem* (2004) **76** (12), 3285.
3. Thaxton, C. S., *et al.*, *Anal Chem* (2005) **77** (24), 8174.
4. Nam, J. M., *et al.*, *J Am Chem Soc* (2004) **126** (19), 5932.
5. Li, T., *et al.*, *Adv Mater* (2009) **22** (2), 286.
6. Hashim, U., *et al.*, *J Eng Res Ed* (2007) **4**, 41.
7. Roy, S., and Gao, Z. Q., *Nano Today* (2009) **4** (4), 318.
8. Lee, J. S., *et al.*, *Biomems and Bionanotech.* (2002) **729**, 185.
9. Lee, J. S., *et al.*, *Micro-TAS* (2002) **1**, 305.
10. Kang, H. K., *et al.*, *7th International Conference on Miniaturized Chemical and Biochemical Analysis Systems* (2003) October 5-9, Squaw Valley, California USA, 697.
11. Choi, Y. K., *et al.*, *J Vac Sci Tech B* (2003) **21** (6), 2951.
12. Roy, S., *et al.*, *J Am Chem Soc* (2009) **131** (34), 12211.
13. Jang, D. Y., *et al.*, *J Vac Sci Tech B* (2007) **25** (2), 443.
14. Porath, D., *et al.*, *Nature* (2000) **403** (6770), 635.
15. Hashioka, S., *et al.*, *J Vac Sci Tech B* (2003) **21** (6), 2937.
16. Hashioka, S., *et al.*, *Appl Phys Lett* (2004) **85** (4), 687.
17. Herne, T. M., and Tarlov, M. J., *J Am Chem Soc* (1997) **119** (38), 8916.
18. Hwang, J. S., *et al.*, *Appl Phys Lett* (2002) **81** (6), 1134.
19. Iqbal, S. M., *et al.*, *Appl Phys Lett* (2005) **86**, .
20. Kim, S. K., *et al.*, *Nanotechnology* (2009) **20** (45), 455502.
21. Liang, X. G., and Chou, S. Y., *Nano Lett* (2008) **8** (5), 1472.
22. Ah, C. S., *et al.*, *Curr Appl Phys* (2006) **6S1**, e157.
23. Sato, T., *et al.*, *J Appl Phys* (1997) **82** (2), 696.
24. Amlani, I., *et al.*, *Appl Phys Lett* (2002) **80** (15), 2761.
25. Park, S. J., *et al.*, *Science* (2002) **295** (5559), 1503.
26. Chung, S. W., *et al.*, *Small* (2005) **1** (1), 64.
27. Piner, R. D., *et al.*, *Science* (1999) **283** (5402), 661.
28. Marcon, L., *et al.*, *Biosens Bioelectron* (2008) **23** (7), 1185.
29. Haguet, V., *et al.*, *Appl Phys Lett* (2004) **84** (7), 1213.
30. Marcon, L., *et al.*, *Bioconjugate Chem* (2008) **19** (4), 802.
31. Zhang, H. J., *et al.*, *Small* (2009) **5** (24), 2797.
32. Kinsella, J. M., and Ivanisevic, A., *Nat Nanotechnol* (2007) **2**, 596.
33. Chen, C. C., *et al.*, *Appl Phys Lett* (2007) **91** (25), 253103.
34. Chang, T. L., *et al.*, *Microelectron Eng* (2007) **84** (5-8), 1698.
35. Chen, C. C., *et al.*, *J Vac Sci Techn B* (2008) **26** (6), 2572.
36. Tsai, C. Y., *et al.*, *Jpn J Appl Phys Part 1-Regular Papers Brief Communications & Review Papers* (2005) **44** (7B), 5711.
37. Cheng, Y. T., *et al.*, *Sens Actuators B-Chem* (2005) **109** (2), 249.
38. Tsai, C. Y., *et al.*, *Microelectron Eng* (2005) **78-79**, 546.
39. Tsai, C. Y., *et al.*, *Appl Phys Lett* (2006) **89** (20), 203902.
40. Cheng, Y. T., *et al.*, *Sens Actuators B-Chem* (2007) **120** (2), 758.
41. Tsai, C. Y., *et al.*, *Microsys Technol* (2005) **11** (2-3), 91.
42. Chang, T. L., *et al.*, *Microelectron Eng* (2006) **83** (4-9), 1630.
43. Chang, T. L., *et al.*, *Biosens Bioelectron* (2007) **22** (12), 3139.
44. Kong, J. M., *et al.*, *Anal Chem* (2008) **80** (19), 7213.
45. Fang, C., *et al.*, *Anal Chem* (2008) **80** (24), 9387.
46. Fan, Y., *et al.*, *J Am Chem Soc* (2007) **129** (17), 5437.
47. Wang, C. J., *et al.*, *Colloids Surf B-Biointerf* (2009) **69** (1), 99.
48. Tokonami, S., *et al.*, *J Electrochem Soc* (2008) **155** (4), J105.
49. Shiigi, H., *et al.*, *J Am Chem Soc* (2005) **127** (10), 3280.
50. Shiigi, H., *et al.*, *Chem Commun (Cambridge, U. K.)* (2003) (9), 1038.
51. Tokonami, S., *et al.*, *Electroanalysis* (2008) **20** (4), 355.
52. Tokonami, S., *et al.*, *Solid State Ionics* (2006) **177** (26-32), 2317.
53. Tokonami, S., *et al.*, *Anal Chem* (2008) **80** (21), 8071.
54. Rutherglen, C., *et al.*, *Nat Nanotechnol* (2009) **4** (12), 811.
55. Guo, X. F., *et al.*, *Science* (2006) **311** (5759), 356.
56. Yagi, I., *et al.*, *Microelectron Eng* (2004) **73-4**, 675.
57. Guo, X. F., *et al.*, *Nat Nanotechnol* (2008) **3** (3), 163.
58. Guo, X. F., *et al.*, *Proc Natl Acad Sci USA* (2006) **103**, 11452.
59. Guo, X. F., and Nuckolls, C., *J Mater Chem* (2009) **19** (31), 5470.
60. Guo, X. F., *et al.*, *Proc Natl Acad Sc. USA* (2009) **106** (3), 691.
61. Qi, P. F., *et al.*, *J Am Chem Soc* (2004) **126** (38), 11774.
62. Whalley, A. C., *et al.*, *J Am Chem Soc* (2007) **129** (42), 12590.
63. Roy, S., *et al.*, *Nano Lett* (2008) **8** (1), 26.
64. Storm, A. J., *et al.*, *Appl Phys Lett* (2001) **79** (23), 3881.
65. Kasumov, A. Y., *et al.*, *Appl Phys Lett* (2004) **84** (6), 1007.
66. Yi, M. Q., *et al.*, *Biosens Bioelectron* (2005) **20** (7), 1320.
67. Ionescu-Zanetti, C., *et al.*, *J Appl Phys* (2006) **99** (2), .
68. Nevill, J. T., *et al.*, *Transducers '05, Digest of Technical Papers, Vol 2* (2005), 1668.
69. Di Carlo, D., *et al.*, *Boston Transducers'03: Digest of Technical Papers, Vol 2* (2003), 1180.
70. Nevill, J. T., *et al.*, *Transducers '05, Digest of Technical Papers, Vol 2* (2005), 1577.
71. Schlecht, U., *et al.*, *Anal Chim Acta* (2006) **573**, 65.
72. Lohndorf, M., *et al.*, *Appl Phys Lett* (2005) **87** (24), .
73. Schlecht, U., *et al.*, *Biosens Bioelectron* (2007) **22** (9-10), 2337.
74. Daniels, J. S., and Pourmand, N., *Electroanalysis* (2007) **19** (12), 1239.
75. Therriault, D., *Nat Nanotechnol* (2007) **2** (7), 393.
76. Maruccio, G., *et al.*, *Analyst* (2009) **134** (12), 2458.
77. Im, H. S., *et al.*, *Nat Nanotechnol* (2007) **2** (7), 430.
78. Sakata, T., *et al.*, *Mater Sci Eng C-Bio S* (2004) **24** (6-8), 827.
79. Kim, D. S., *et al.*, *Sens Actuators B-Chem* (2006) **117** (2), 488.
80. Gu, B., *et al.*, *Small* (2009) **5** (21), 2407.
81. Kim, C. H., *et al.*, *Biochip J* (2008) **2** (2), 127.
82. Groeseneken, G., *et al.*, *IEEE Trans Electron Devices* (1984) **31** (1), 42.
83. Kim, S., *et al.*, *Appl Phys Lett* (2009) **94** (24), 243903.